

SCIENTIFIC REPORTS



OPEN

Astrocytic Acid-Sensing Ion Channel 1a Contributes to the Development of Chronic Epileptogenesis

Feng Yang^{1,*}, Xiaolong Sun^{1,*}, Yinxiu Ding^{1,2,*}, Hui Ma¹, Tangpeng OuYang¹, Yue Ma¹, Dong Wei¹, Wen Li¹, Tianle Xu³ & Wen Jiang¹

Received: 02 April 2016
Accepted: 26 July 2016
Published: 16 August 2016

Unraveling mechanisms underlying epileptogenesis after brain injury is an unmet medical challenge. Although histopathological studies have revealed that reactive astrogliosis and tissue acidosis are prominent features in epileptogenic foci, their roles in epileptogenesis remain unclear. Here, we explored whether astrocytic acid-sensing ion channel-1a (ASIC1a) contributes to the development of chronic epilepsy. High levels of ASIC1a were measured in reactive astrocytes in the hippocampi of patients with temporal lobe epilepsy (TLE) and epileptic mice. Extracellular acidosis caused a significant Ca^{2+} influx in cultured astrocytes, and this influx was sensitive to inhibition by the ASIC1a-specific blocker psalmotoxin 1 (PcTX1). In addition, recombinant adeno-associated virus (rAAV) vectors carrying a GFAP promoter in conjunction with ASIC1a shRNA or cDNA were generated to suppress or restore, respectively, ASIC1a expression in astrocytes. Injection of rAAV-ASIC1a-shRNA into the dentate gyrus of the wide type TLE mouse model resulted in the inhibition of astrocytic ASIC1a expression and a reduction in spontaneous seizures. By contrast, rAAV-ASIC1a-cDNA restored astrocytic ASIC1a expression in an ASIC1a knock-out TLE mouse model and increased the frequency of spontaneous seizures. Taken together, our results reveal that astrocytic ASIC1a may be an attractive new target for the treatment of epilepsy.

Epilepsy, characterized by a predisposition for unpredictable seizures, affects approximately 50 million people worldwide, making it one of the most frequently occurring brain diseases¹. Despite the current availability of over two dozen antiepileptic drugs (AEDs), about one-third of patients with epilepsy still have poor seizure control and become medically refractory epilepsy². Moreover, the currently available AEDs are primarily intended to suppress epileptic seizures and, therefore, only treat symptoms rather than cure patients of epilepsy by targeting the underlying pathology². Thus, a deeper understanding of the mechanisms involved in the etiology of epilepsy may help identify novel therapeutic targets for its prevention and treatment.

Epileptogenesis, the process by which the normal brain develops epilepsy, involves a number of alterations in molecular, cellular and neuronal networks¹. Studies on epileptogenic foci removed by surgical resection from human brain tissue have suggested an important role for astrocytes in epileptogenesis³. For example, reactive astrogliosis is one of the most common pathological characteristics in the sclerotic hippocampi of patients with mesial temporal lobe epilepsy (TLE)⁴. The abnormal expression and distribution of certain G-protein coupled receptors and voltage gated ion channels on the surface of reactive astrocytes may lead to excessive intracellular Ca^{2+} accumulation that has the potential to then spread to adjacent astrocytes in the form of a “calcium wave”. Simultaneously, this Ca^{2+} accumulation promotes the release of gliotransmitters, including the excitatory transmitters glutamate and ATP, and, thus, contributes to the generation and spread of seizure activity^{3,5,6}. In addition to astrogliosis, chronic inflammation has been observed in epileptic human brain tissue^{7,8}. Along these lines, recent evidence suggests that inflammation is also an important factor in the initiation of seizures and

¹Department of Neurology, Xijing Hospital, the Fourth Military Medical University, Xi'an 710032, China. ²The Key Laboratory of Cerebrocranial Diseases, Ningxia Medical University, Yinchuan 750004, China. ³Department of Anatomy, Histology and Embryology, Collaborative Innovation Center for Brain Science, Shanghai Jiao Tong University School of Medicine, Shanghai, 200025, China. *These authors contributed equally to this work. Correspondence and requests for materials should be addressed to W.J. (email: jiangwen@fmmu.edu.cn)

epileptogenesis^{9,10}. However, the mechanisms underlying epileptogenesis and the role of inflammation are not yet fully understood.

One important aspect of inflammation is tissue acidosis, where the extracellular pH drops as low as 5.4^{11–13}. Low pH activates a unique family of acid-sensing ion channels (ASICs), which are voltage-independent, proton-gated cation-selective channels belonging to the degenerin/epithelial Na⁺ channel (DEG/ENaC) superfamily¹⁴. While many ASICs are largely Ca²⁺ impermeable, homomeric ASIC1a is Ca²⁺-permeable and highly sensitive to protons, making it a particularly interesting candidate to study in the context of epilepsy^{15,16}. ASIC1a is widely expressed throughout the central nervous system, especially in the amygdala, hippocampus, cingulate cortex, somatosensory cortex, striatum and periaqueductal gray, and has functional implications in synaptic plasticity, learning and memory^{17–19}. Our recent pilot experiment revealed that reactive astrocytes in the sclerotic hippocampi of epileptic mice express ASIC1a at high levels. Therefore, we hypothesized that ASIC1a in reactive astrocytes may contribute to the development of chronic epileptogenesis.

Accordingly, in this study, we first measured the expression of ASIC1a in the sclerotic hippocampi of epileptic mice and TLE patients, as well as in lipopolysaccharide (LPS)-activated astrocytes *in vitro*. Next, the effect of ASIC1a activation on intracellular Ca²⁺ levels in reactive astrocytes was determined *in vitro*. Last, the role of hippocampal astrocytic ASIC1a in the development of chronic epileptogenesis was examined by down-regulating and restoring ASIC1a expression in reactive astrocytes of wild-type mice and ASIC1a knock-out (ASIC1a^{-/-}) mice, respectively.

Results

High levels of ASIC1a expression in hippocampal reactive astrocytes of epileptic mice and TLE patients.

It has been recently reported that ASIC1a is expressed in astrocytes in normal brain tissue²⁰. However, its expression profile in the epileptic brain has not been elucidated. Therefore, we first examined the co-expression of ASIC1a and Glial fibrillary acidic protein (GFAP, a marker of astrocytes) in the mouse hippocampus at 3, 7, and 28 days after SE. In the dentate gyrus, the number of astrocytes at 3 days post-SE was significantly greater than control. On day 7, astrocyte numbers were still elevated compared to control, but decreased slightly compared to day 3. On day 28, astrocyte number declined to control levels ($P > 0.05$) (Fig. 1a,b). However, the ratio of astrocytes expressing ASIC1a increased significantly from day 3 to day 28 (42% and 78%, respectively), and was significantly elevated in all post-SE groups compared to control (Fig. 1c) ($P < 0.001$). To investigate the precise subcellular localization of ASIC1a in the dentate gyrus, electron microscopy was performed. Very little ASIC1a was expressed on the thin (non-reactive) astrocytic processes in control mice (Fig. 1d). While in epileptic mice (28 days post-SE), ASIC1a was abundant in the hypertrophic cellular processes of reactive astrocytes (Fig. 1e). These data suggest that, in sclerotic hippocampi, ASIC1a expression is significantly up-regulated in reactive astrocytes.

To confirm the expression of astrocytic ASIC1a in human brain, we double-labeled GFAP and ASIC1a in the sclerotic hippocampal tissue resected from TLE patients and control (traumatic brain injury caused by car accidents) patients. There was only a faint expression of ASIC1a on the hippocampal astrocytes in the control patients (Fig. 2a1–a4), with most located on neuron-like cells (Fig. 2a2), which was consistent with previous report²⁰. While in the TLE patients, ASIC1a was abundantly expressed in hippocampal activated astrocytes, which displayed hypertrophy of cell bodies and processes (Fig. 2b1–b4). Interestingly, ASIC1a was mainly located in membrane and cytoplasm of reactive astrocytes. Because the hippocampal resections were incomplete, hippocampal subfields could not be identified.

Increased ASIC1a expression in cultured astrocytes. To further confirm the upregulation of ASIC1a in reactive astrocytes, primary astrocytes were treated with LPS (2 µg/ml), an inflammatory stimulus, to mimic reactive astrocytes *in vivo*. Immunofluorescence and western blot were performed to detect the ASIC1a expression. Compared with the untreated control group, at 24 hours after LPS pretreatment, astrocytes were hypertrophied and showed thicker ASIC1a and GFAP-positive staining (Fig. 3a). Also, immunoblot analysis showed that, compared to control, total and membrane ASIC1a protein levels were elevated at 24 and 48 (but not 8) hours after LPS treatment (Fig. 3b,c).

ASIC1a-mediated Ca²⁺ elevation in cultured astrocytes. ASIC1a activation allows high levels of Ca²⁺ influx²¹. We therefore explored whether ASIC1a activation affects intracellular Ca²⁺ levels in reactive astrocytes. Astrocytes were activated by pre-treatment with LPS (2 µg/ml) for 24 hours. Ca²⁺ imaging showed that the intracellular Ca²⁺ concentration increased when the extracellular pH was reduced from 7.4 to 6.0, which could be partially abolished by the ASIC1a-specific antagonist psalmotoxin 1 (PcTx1) (5 nM) (Fig. 3d). The matching traces were plotted in Fig. 3e. Reducing the pH to 6.0 caused a transient increase of normalized fluorescence intensity to $64.0 \pm 10.4\%$ above baseline (F/F_0 max, $n = 24$, Fig. 3e) with a long lasting decrease. Co-application of PcTx1 attenuated this increase to $11.3 \pm 12.5\%$ above baseline (F/F_0 max, $n = 21$, Fig. 3e), suggesting that PcTx1 significantly suppressed the acid-induced Ca²⁺ influx. Therefore, the acid-induced elevation of astrocytic Ca²⁺ is mediated, at least in part, by ASIC1a channels.

Efficiency of viral transduction. The efficiency of viral ASIC1a transgene expression was first examined using cultured astrocytes from WT mice at 72 hours after virus transduction. Astrocytes were imaged for reporter Enhanced green fluorescent protein (EGFP) fluorescence. As shown in Fig. 4e–h, the ratios of EGFP-positive astrocytes were $96.6 \pm 1.2\%$ in rAAV-ASIC1a-scramble group, $94.5 \pm 1.5\%$ in rAAV-ASIC1a-shRNA group, $95.8 \pm 1.8\%$ in rAAV-empty group, and $93.6 \pm 1.1\%$ in rAAV-ASIC1a group, respectively. There were no differences between groups (data not shown). The efficiency of viral transduction was then verified by western blot. rAAV-ASIC1a-shRNA markedly reduced the expression of ASIC1a compared to rAAV-ASIC1a-scramble

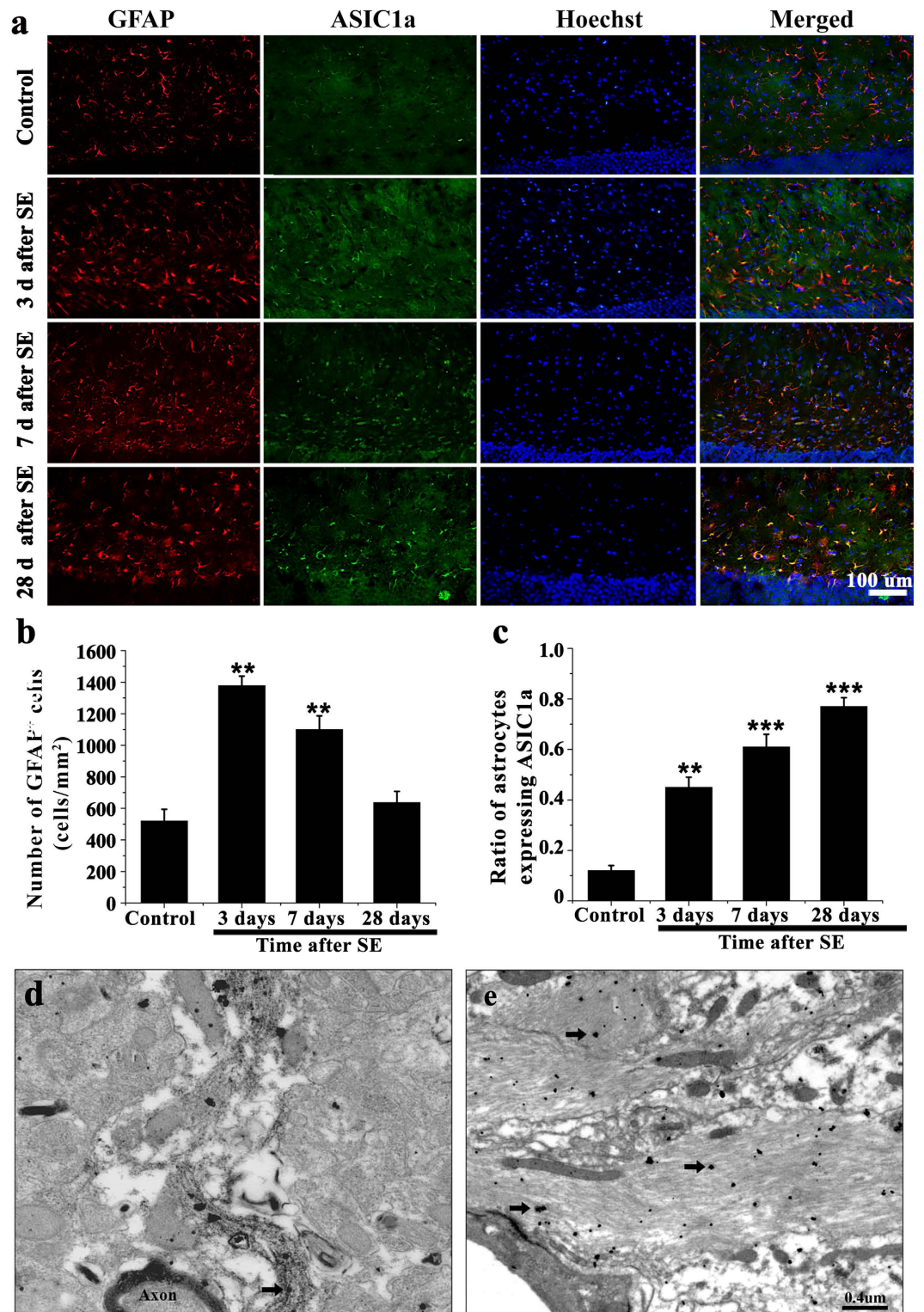


Figure 1. ASIC1a was abundantly expressed in hippocampal astrocytes of epileptic mice. (a) GFAP (red), ASIC1a (green), and Hoechst (blue) immunofluorescence staining was performed on control tissue and at 3, 7, and 28 days after SE. (b) The number of GFAP positive cells peaked on day 3 after SE. $**P < 0.01$, ANOVA followed by Dunnett's post-hoc test vs. control. (c) The fraction of astrocytes expressing ASIC1a increased between 3 and 28 days after SE. $**P < 0.01$, $***P < 0.001$; ANOVA followed by Dunnett's post-hoc test vs. control. (d,e) Electron microscopy showed astrocytic ASIC1a (black arrow) in control (d) and epileptic (28 days after SE) (e) mice.

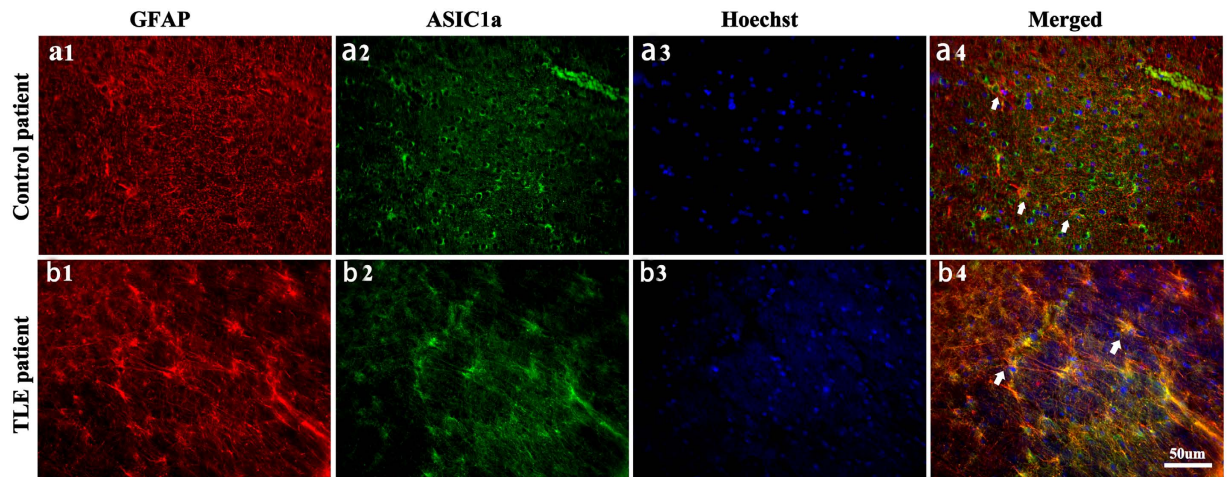


Figure 2. ASIC1a was abundantly expressed in hippocampal astrocytes of TLE patients. (a1–b4) GFAP (red), ASIC1a (green), and Hoechst (blue) immunofluorescence staining was performed on TLE patients and control (traumatic brain injury caused by car accidents) patients. (a1–a4) There was only a faint expression of ASIC1a on the hippocampal astrocyte in the 4 cases of control patients, with more seeming to be located on neuron-like cells. (b1–b4) In all the 4 cases of TLE patients, ASIC1a was abundantly expressed in activated hippocampal astrocytes, which displayed hypertrophy of cell bodies and processes.

(Fig. 4i,j). ASIC1a expression was significantly higher in rAAV-ASIC1a than in rAAV-empty-infected cells (Fig. 4k,l).

We then examined viral expression in injected hippocampi of WT and KO mice. AAV-mediated gene expression is reported to peak at 3–4 weeks *in vivo*²². Therefore, we examined ASIC1a expression at 4 weeks after virus injection (5 weeks after SE). To minimize viral injection lesions, a single injection point in each dentate gyrus was used. Low magnification images of the hippocampus (Fig. 5c) showed EGFP fluorescence around projection areas, covering over almost all the dentate gyrus. EGFP fluorescence was mainly localized to the polymorph and molecular layers. Weak EGFP fluorescence extended into CA1. Quantification of the co-expression of ASIC1a and EGFP showed that in WT mice, rAAV-ASIC1a-shRNA significantly reduced EGFP and ASIC1a co-expression compared to rAAV-ASIC1a-scramble ($57.8 \pm 2.6\%$ and $76.4 \pm 3.2\%$, respectively); In KO mice, rAAV-ASIC1a rescued ASIC1a expression in $61.1 \pm 1.7\%$ of EGFP positive cells; ASIC1a was absent in EGFP-positive cells from KO mice injected with the rAAV-empty vector (Fig. 5a,b). These results indicated that our viral vectors can efficiently transduce widespread ASIC1a transgene expression in astrocytes *in vivo* and *in vitro*.

The role of astrocytic ASIC1a in chronic epileptogenesis. Lastly, we tried to examine the effects of manipulating hippocampal astrocytic ASIC1a on chronic epileptogenesis. We down-regulated and restored ASIC1a expression in astrocytes of WT and KO mice, respectively, and examined spontaneous seizures during the 5th week after SE. Every spontaneous seizure was carefully confirmed by behavioral features associated with ictal events in EEG recording. Representative ictal EEG recordings of each group were shown in Fig. 6a.

In WT mice, video-EEG analysis showed that seizure frequency in the rAAV-ASIC1a-shRNA group (1.27 ± 0.3 seizures/12 h, $n = 6$) was lower than the rAAV-ASIC1a-scramble group (1.79 ± 0.4 seizures/12 h, $n = 6$) ($P < 0.05$). In KO mice, seizure frequency in the rAAV-ASIC1a group (1.31 ± 0.3 seizures/12 h, $n = 7$) was higher than the rAAV-empty group (0.89 ± 0.3 seizures/12 h, $n = 7$) ($P < 0.05$) (Fig. 6b,c). No differences in seizure score or average duration of spontaneous seizures were observed between groups ($P > 0.05$) (Fig. 6d,e). Taken together, these results suggested that down-regulation of astrocytic ASIC1a expression in WT mice decreased spontaneous seizures frequency in chronic period of epileptogenesis, while restored the expression of astrocytic ASIC1a in KO mice had the opposite effect.

Discussion

In this study, we uncovered the following four findings. First, high ASIC1a levels are expressed on reactive astrocytes in the hippocampi of both TLE patients and epileptic mice, as well as in LPS-induced reactive astrocytes *in vitro*. Second, activation of ASIC1a results in a significant increase of intracellular Ca^{2+} levels in reactive astrocytes. Third, down-regulation of astrocytic ASIC1a in the epileptic hippocampi of WT mice inhibits spontaneous seizures. Fourth, restoration of astrocytic ASIC1a expression in the epileptic hippocampi of ASIC1a KO mice increases the frequency of spontaneous seizures. These results provide the first direct evidence that astrocytic ASIC1a is an important contributing factor in the development of epileptogenesis.

Astrocytes, the most abundant glial cell type in the mammalian brain, play essential roles in brain pathophysiology through modulation of synaptic transmission and regulation of ion homeostasis and blood–brain barrier integrity²³. These cells respond to a range of brain insults through a complex process referred to as reactive astrogliosis. This process involves both morphological and functional changes, including hypertrophy, increased proliferation, and up-regulation of intermediate filaments, such as GFAP²⁴. In this study, significant reactive astrogliosis was discovered in the hippocampus during epileptogenesis induced by pilocarpine, which was consistent

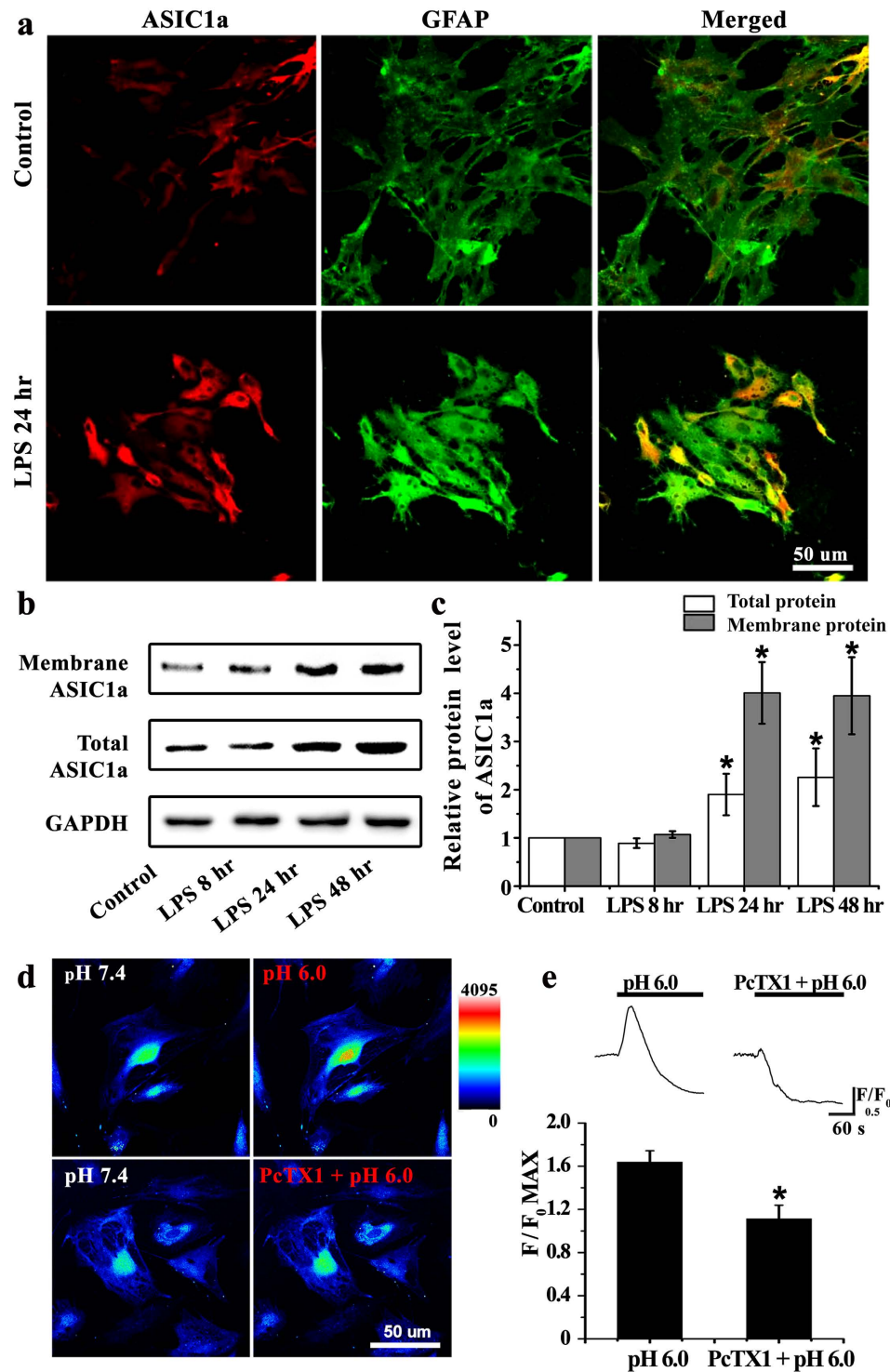


Figure 3. Increased expression of astrocytic ASIC1a mediated Ca^{2+} elevation in LPS-treated astrocytes. (a) ASIC1a (red) and GFAP (green) immunofluorescence staining was performed in cultured astrocytes. Compared with the control group, the number of ASIC1a-positive astrocytes markedly increased at 24 hours after LPS treatment. (b) Western blots for membrane and total ASIC1a protein in control and LPS-treated astrocytes at 8, 24, and 48 hours after treatment. (c) Densitometric quantification of the membrane and total ASIC1a protein expression, normalized to GAPDH. * $P < 0.05$, ANOVA followed by Dunnett's post-hoc test vs. control. (d) Representative changes of intracellular Ca^{2+} concentration in response to extracellular pH reduction (from 7.4 to 6.0) in the absence and presence of 5 nM PcTX1. Warmer colors indicated higher fluorescence intensity. (e) Time course and quantification of fluorescence intensity. Peak fluorescence intensity was normalized to fluorescence intensity at baseline (F/F_0 max) in the pH 6.0 ($n = 24$) and PcTX1 + pH 6.0 ($n = 21$) groups. * $P < 0.05$, t test vs. pH 6.0 group.

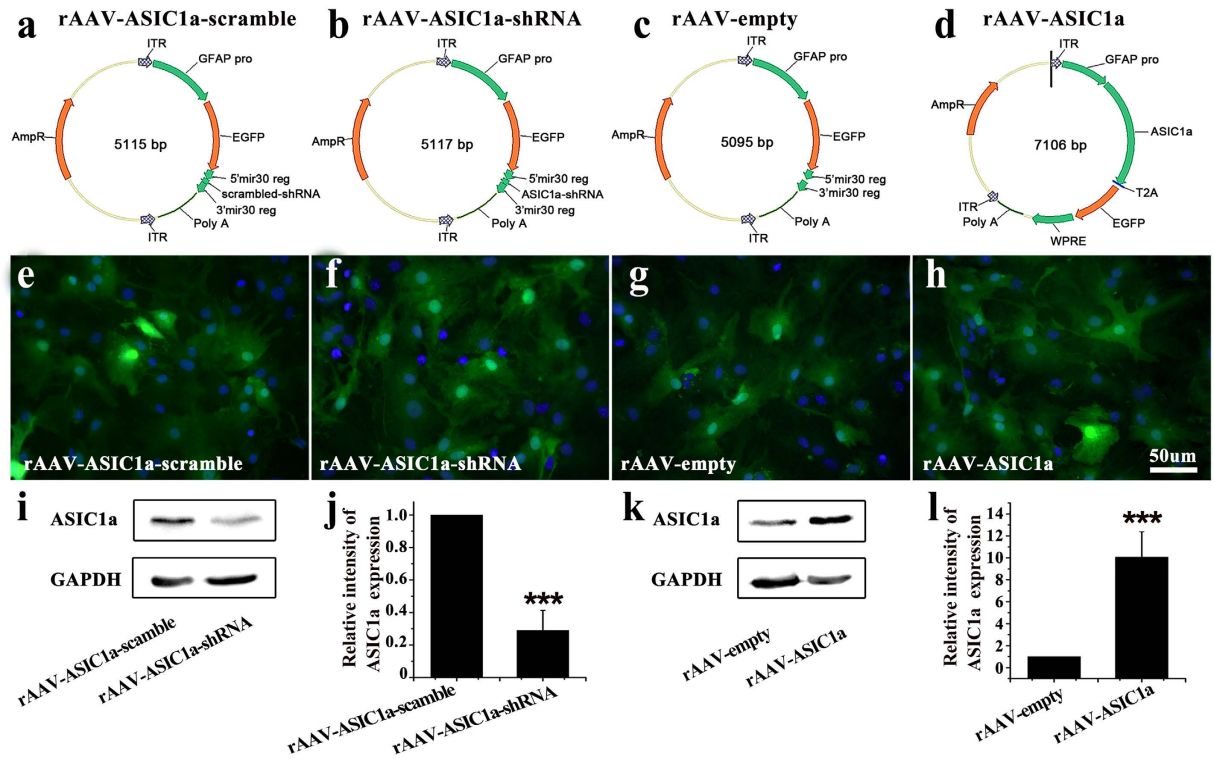


Figure 4. rAAV plasmids and virally induced ASIC1a expression in cultured astrocytes. (a–d) Schematic of the four rAAV plasmids used: rAAV-ASIC1a-scramble virus carrying a GFAP-EGFP-ASIC1a-scrambled-shRNA vector, rAAV-ASIC1a virus carrying a GFAP-EGFP-ASIC1a-shRNA vector, rAAV-empty virus carrying a GFAP-EGFP vector, and rAAV-ASIC1a virus carrying GFAP-ASIC1a-EGFP vector. (e–h) EGFP and Hoechst fluorescence in astrocyte cultures at 72 hours after virus transduction. (i, k) Immunoblots for total ASIC1a protein after viral transduction. (j, l) Densitometric quantification of ASIC1a, normalized to GAPDH. *** $P < 0.001$, t test vs. scramble or empty vector.

with our previous study²⁵. Reactive astrocytes may contribute to epileptogenesis by losing normal or gaining abnormal astrocytic functions²⁶. For example, Eid *T et al.* noted a reduction in the expression of water channel aquaporin 4 and dystrophin on reactive astrocytes in the sclerosis hippocampus of TLE patients. This may result in a perturbed water flux through astrocytes, which can lead to impaired buffering of K^+ and an increased propensity for seizures²⁷. In this work, we provide the first report of high levels of ASIC1a on reactive astrocytes in the sclerosis hippocampus of epileptic mice and TLE patients.

ASIC1a is a member of a novel family of proton-gated amiloride-sensitive cation channels and is expressed primarily in Ca^{2+} and Na^+ permeable neurons¹⁴. Activation of these channels results in intracellular Ca^{2+} accumulation, which plays an important role in neurological disorders, such as brain ischemia, multiple sclerosis and spinal cord injury¹⁴. Recently, Huang *C et al.* found ASIC1 was expressed in cultured and *in situ* astrocytes. Specifically, ASICs were mainly expressed in the nucleus, but not in the membrane/cytoplasm, of astrocytes under physiological condition²⁰. In this study, high levels of ASIC1a were found in the membrane/cytoplasm of reactive astrocytes under pathological conditions, suggesting possible trafficking of ASICs in astrocytes in response to certain stimuli. *In vitro* experiments further indicate that astrocytic ASIC1a can sense extracellular acidosis and mediate Ca^{2+} influx, confirming that ASIC1a in the membrane of astrocytes is functional. It is interesting to observe a long-lasting decline of intracellular Ca^{2+} following the transient increase when lowering extracellular pH from 7.4 to 6.0. This phenomenon is likely to be associated with 1) gap junctions between astrocytes, which cause the intercellular propagation of calcium wave, and 2) our experimental conditions, including lifetime of calcium indicators, environment of the laboratory, cell's state, and so on.

Astrocytic Ca^{2+} signaling plays a pivotal role in communication between astrocytes and neurons²⁸. Several lines of evidence indicate that activation of Ca^{2+} signals in astrocytes induces the subsequent release of gliotransmitters, such as glutamate, D-serine, and ATP, which may amplify the propensity for epileptic seizures⁶. In this study, it was found that ASIC1a activation in reactive astrocytes resulted in a significant elevation in cytosolic Ca^{2+} levels. Study *in vivo* revealed that inhibiting astrocytic ASIC1a expression in the sclerotic hippocampus using a rAAV carrying ASIC1a shRNA reduced the frequency of spontaneous seizures. Furthermore, restoring astrocytic ASIC1a expression in the sclerotic hippocampus of ASIC1a knock-out mice using a rAAV carrying ASIC1a cDNA displayed the opposite phenotype. These results suggest that astrocytic ASIC1a activation increases the excitability of the hippocampal local circuit and contributes to the development of epileptogenesis. However, the detailed mechanisms linking astrocytic ASIC1a activation and neuronal hyperexcitability require further delineation.

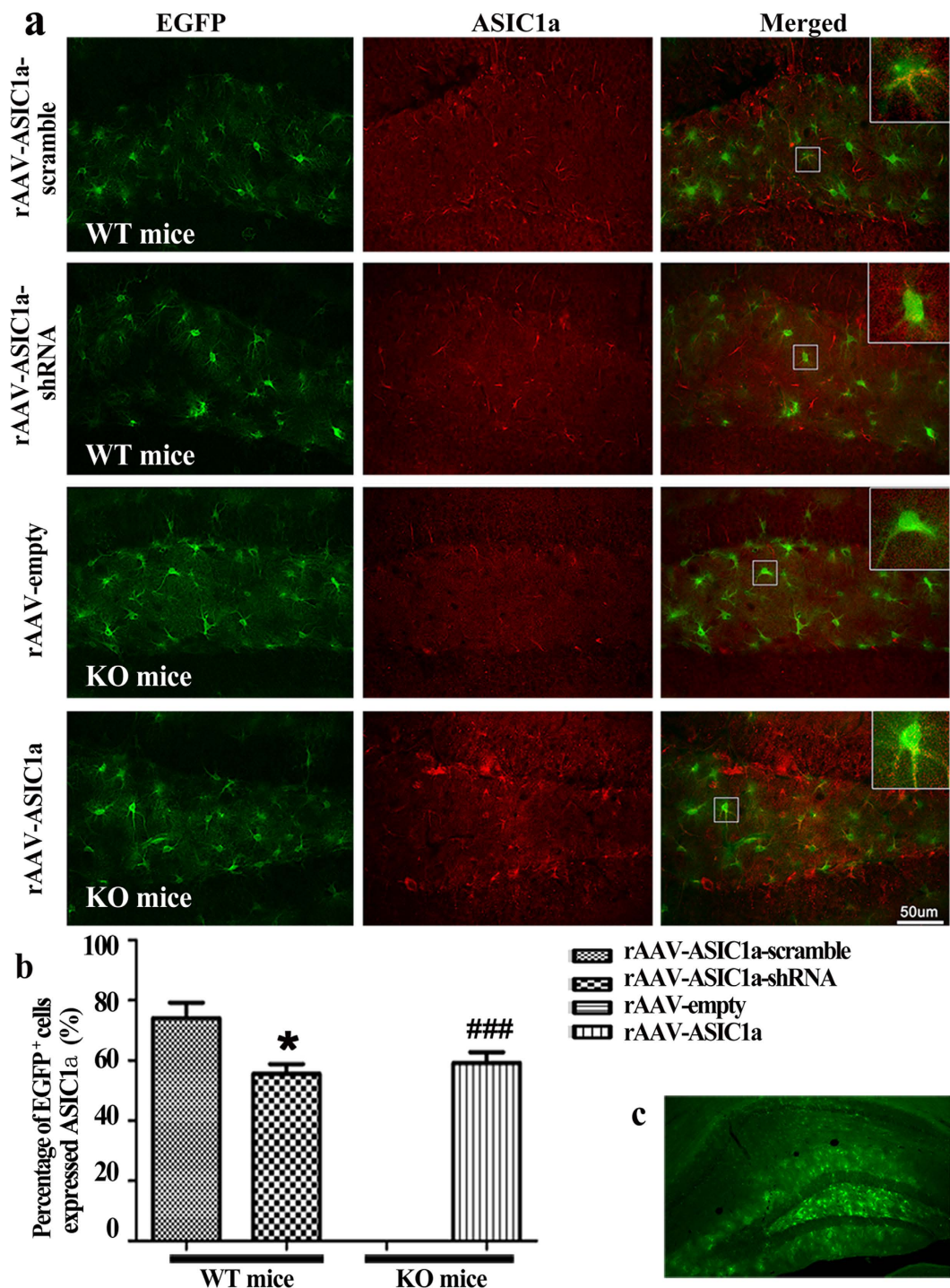


Figure 5. The efficiency of viral vector-induced ASIC1a expression at 5 weeks after SE. (a) EGFP and ASIC1a immunofluorescence staining in each group. (b) Percent of EGFP-positive cells expressing ASIC1a in each group. All data were shown as mean \pm SEM. WT: n = 7, KO: n = 6 mice per group. * $P < 0.05$, t test vs. rAAV-ASIC1a-scramble; ### $P < 0.001$, t test vs rAAV-empty. (c) Low magnification view showing the region of virus transduction in the dentate gyrus.

In the literature, the exact roles of ASICs in seizure generation, propagation and termination have been controversial²⁹. A number of *in vivo* studies have found amiloride, a commonly used non-selective ASIC blocker, has an anticonvulsant effect in pilocarpine, pentylenetetrazole and febrile seizure models^{30–33}. In addition, some *in vitro* studies revealed that ASIC1 activation might be proconvulsant in a cell culture model of epilepsy and in hippocampal slices²⁹. However, Ziemann and colleagues found that ASIC1a activation was involved in the termination of epileptic seizure activity because ASIC1a expression levels were higher in GABAergic interneurons than in excitatory neurons³⁴. From this it was concluded that ASIC1a activation limited seizures by increasing

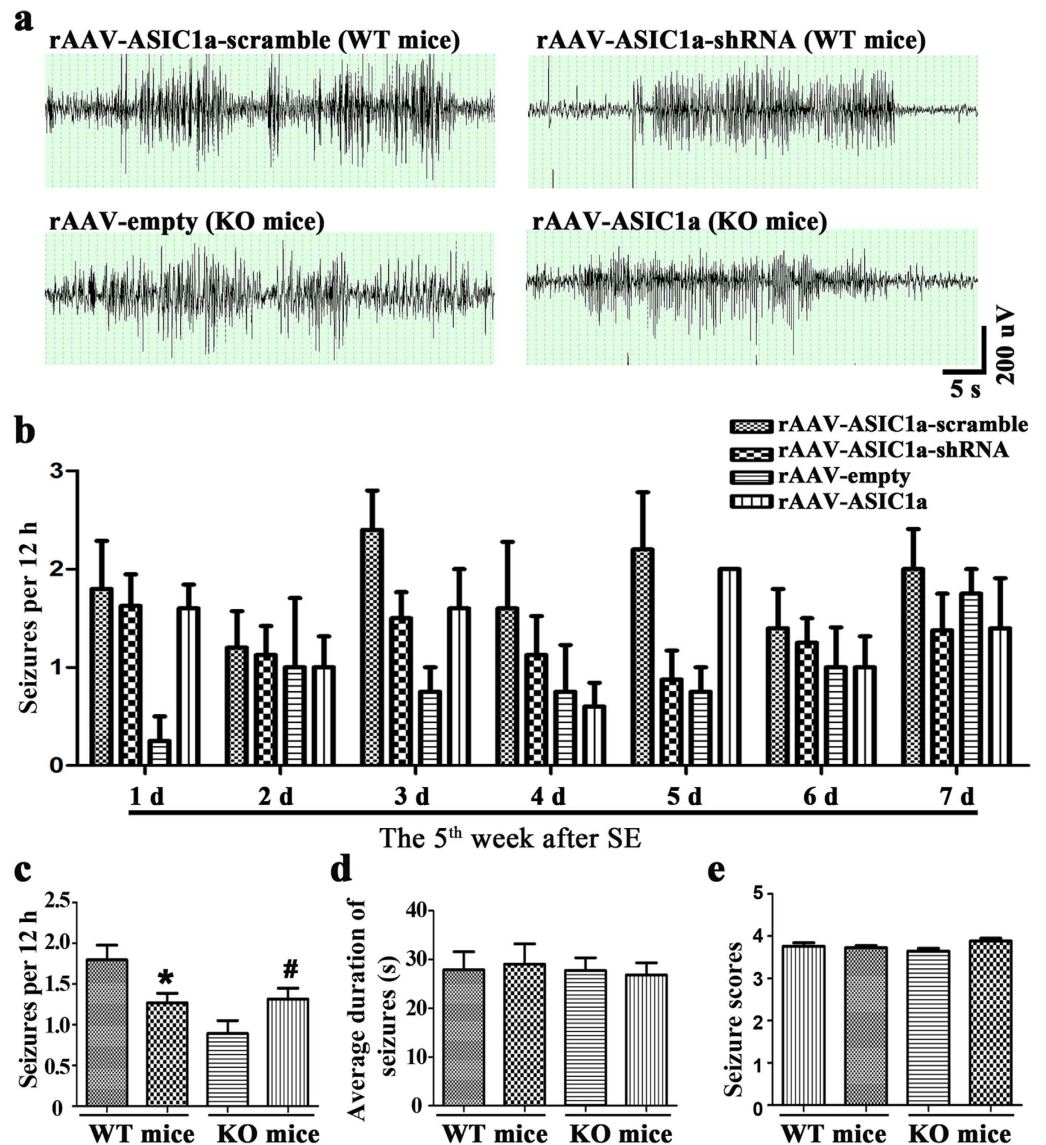


Figure 6. Effects of rAAV vectors on spontaneous seizures in mice during chronic epileptogenesis. (a) Ictal EEG signals in each group. (b) Spontaneous seizure frequency during the 5th week after SE. (c–e) Statistical analysis of spontaneous seizure frequency, total time in seizures, and seizure scores. * $P < 0.05$, t test vs. rAAV ASIC1a-scramble. # $P < 0.05$, t test vs. rAAV-empty. Bars represent mean \pm SEM. WT: $n = 7$, KO: $n = 6$ mice/group.

inhibitory tone. In this paper, we focused on the development of chronic epileptogenesis, during which period reactive astrogliosis and significant loss of GABAergic interneurons predominate^{35–37}. Expression of ASIC1a channels was abundant in reactive astrocytes, and activation of these channels led to the elevation of intracellular Ca^{2+} concentrations, and, thus, contributed to the development of chronic epileptogenesis. In fact, ASIC1a channels in both neurons and astrocytes could be activated simultaneously when acidosis occurs in the same tissue. The influence of ASIC1a on the neural network depends on the integrated effects of ASIC1a on different neuronal cells. So, due to the imbalance of ASIC1a expressions on reactive astrocytes and GABAergic interneurons, the effect of ASIC1a on neural network in chronic epileptogenesis may depend on hyper-excitability mediated by reactive astrocytes. Therefore, our study is not in conflict with the results published by Ziemann and colleagues. Rather, this work contributes to our understanding of ASIC1a functions in epilepsy.

ASICs belong to the DEG/ENaC superfamily¹⁷. To date, there are seven subunits of ASICs (1a, 1b1, 1b2, 2a, 2b, 3, and 4) that have been identified, which are encoded by four genes¹¹. Besides ASIC1a, several other ASIC subunits have been reported to have a role in epileptic seizures. Wu H *et al.* found that pilocarpine-induced seizures were associated with significant up-regulation of ASIC2a in the piriform cortex, and that inhibition of ASICs, particularly ASIC2a, suppressed seizures originating in this region³⁸. Cao Q *et al.* reported that ASIC3 expression was elevated in TLE patient and epileptic rat brains, and co-localized with astrocyte marker GFAP and inhibitory GABAergic interneuron marker GAD67. Intracerebroventricular injection of the ASIC3 inhibitor APETx2

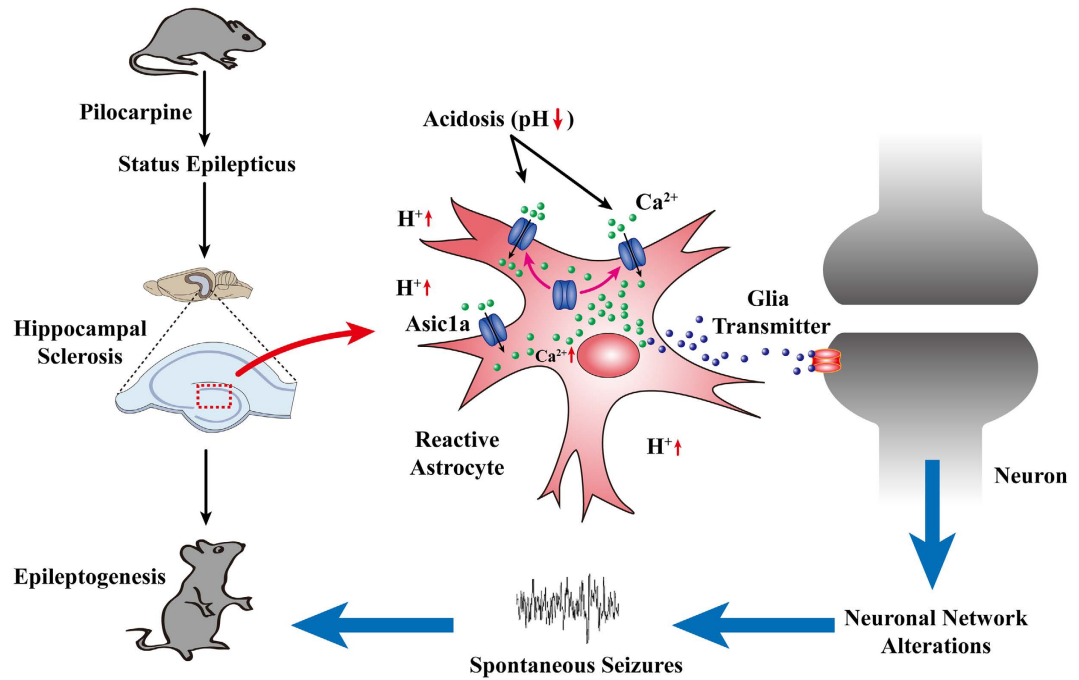


Figure 7. Proposed role of astrocytic ASIC1a in chronic epileptogenesis. Acute brain injury such as status epilepticus can cause hippocampal sclerosis. Reactive astrogliosis and tissue acidosis are the prominent features in sclerotic hippocampi. Reactive astrocytes express a high level of ASIC1a, which can be activated by local extracellular low pH. This would lead to excessive Ca^{2+} influx in astrocytes and release of gliotransmitters, thus resulting in epileptiform activities and the development of chronic epileptogenesis.

shortened the latency to seizure and increased the incidence of generalized tonic clonic seizure in experimental epilepsy models, suggesting that elevated levels of ASIC3 may be antiepileptic³⁹. However, studies remain to be conducted on whether reactive astrocytes in the sclerosis hippocampus abundantly express ASIC2a and/or ASIC3 and what is these channels' function in this context.

To elucidate the role of astrocytic ASICs in brain function, it is necessary to manipulate their expression *in situ* where neuronal/glia interactions remain intact. Such manipulations include molecular genetics, imaging, and use of transgenic animals. However, these approaches are technically challenging, time consuming, and have variables that are difficult to control⁴⁰. Gene transfer is a valuable method by which to target astrocytes and explore their functions in experimental disease models. In particular, viral-mediated gene transfer is a rapid, flexible and cost-effective *in vivo* technique that can be used to investigate the function of genes of interest in adult brains⁴¹. The rAAV vector in particular is commonly used both *in vivo* and *in vitro* due to its high efficiency, stability, minimal immunogenicity, and broad host and cell range⁴². In this study, we employed high-titer AAV2 vectors carrying a 682 bp GFAP promoter, an efficient and specific method to regulate gene expression in astrocytes⁴³.

Although the present study has yielded some important findings concerning ASIC1a and its role in epileptogenesis, some limitations should be noted. First, the rAAV vectors used to manipulate astrocytic ASIC1a expression were only transduced into the dentate gyrus of the sclerotic hippocampi, which might be insufficient to cover all of the epileptogenic regions in the pilocarpine TLE model⁴⁴. This could, at least in part, be the reason that inhibition of astrocytic ASIC1a reduced, but failed to completely abrogate, spontaneous seizures. Second, continuous video-EEG monitoring and behavioral observation were performed for a maximum of seven days. Although statistically significant differences were found in the frequency of spontaneous seizures among the different experimental groups within this timeframe, there is a cyclicity of spontaneous recurrent seizures in the pilocarpine TLE model⁴⁵ that warrants longer behavioral and EEG monitoring in the future studies. Third, further investigations are needed to elucidate the deeper *in vivo* underlying mechanism of epileptogenesis induced by astrocytic ASIC1a activation.

In conclusion, our study revealed that astrocytic ASIC1a plays a vital role in epileptogenesis (Fig. 7) and has the potential to serve as a novel target for the treatment of epilepsy.

Materials and Methods

Animals. Wild-type (WT) and ASIC1a knock-out (KO) mice weighing 20–25 g were used. Mice were maintained on a congenic C57BL/6 background. Animals were housed at 24–25 °C and 50–60% humidity on a 12-hour light/dark cycle (lights on at 8:00 A.M.). Food and water were provided *ad libitum*. All experimental procedures were approved by the Fourth Military Medical University Animal Care Committee in strict accordance with the guidelines established by the US National Institutes of Health.

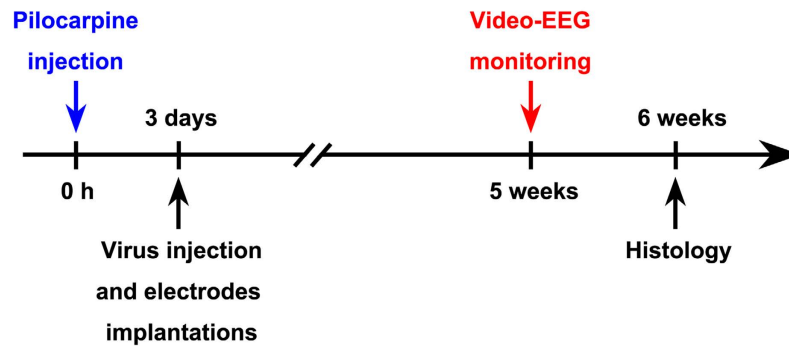


Figure 8. The flow chart of pilocarpine injection, virus injection and electrodes implantations, video-EEG monitoring and histology for Experiment 2 in the Materials and Methods.

rAAV-vector production. We specifically targeted astrocytes using a recombinant AAV2 vector carrying a 682-bp mouse GFAP promoter⁴³. The construction and production of vectors were performed as our previous study^{43,46,47}. The shRNA targeting mouse ASIC1a was designed as follows: 5'-TCGACTATGCCTATGAGGTCATTAACCTCGAGAATGACCTCATAGGCATAGTCTTTTTT-3' (bold: shRNA-sense and -antisense strands, respectively; italics: hairpin turn). The control (scrambled) shRNA sequence was: 5'-TCGATTCTCCGAACGTGTCACGTTTCAAGAGAACGTGACIACGTTCCGGAGAATTTTTTG-3'. ASIC1a-shRNA, ASIC1a-scramble or ASIC1a-cDNA was subcloned into an expression cassette consisting of the mouse GFAP promoter. EGFP was used as a reporter gene. The recombinant plasmid was identified by DNA sequencing (Fig. 4a–d).

Pilocarpine-induced SE. To induce status epilepticus (SE), a single dose of pilocarpine (130 mg/kg, i.p., Sigma) was given at 18 hours after lithium chloride (350 mg/kg, i.p., Sigma) administration. After 60 minutes SE, seizures were terminated with diazepam (30 mg/kg, i.p.). Subjects were closely observed during SE and given supportive care (food soaked in a 5% glucose solution for 3 days) until normal eating and drinking behavior resumed.

This study consisted of two experiments with specific aims. Experiment 1 aimed to examine the expression pattern of astrocytic ASIC1a in epileptogenesis. WT mice were divided into two groups. Group 1 ($n = 5$) comprised the control group, which did not undergo SE. SE was induced in group 2 ($n = 24$) animals. Of the 24 mice injected with LiCl-pilocarpine, 22 mice developed SE, and 4 mice died during or shortly after SE. The remaining 18 mice were perfused for histology 3, 7, and 28 days after SE ($n = 6$ for each time point), respectively.

Experiment 2 aimed to investigate the role of astrocytic ASIC1a in epileptogenesis. 20 WT and 20 KO mice received LiCl-pilocarpine to induce SE. 18 WT and 17 KO mice developed SE. Of these, 4 WT and 5 KO mice died during or shortly after SE. The flowchart of experimental 2 procedure was shown as in Fig. 8.

rAAV-vector injection and EEG electrode implantation. Three days after SE, WT mice in experiment 2 were randomly assigned to 2 groups, receiving bilateral hippocampal injections of either rAAV-ASIC1a-scramble or rAAV-ASIC1a-shRNA ($n = 7$ /group). KO mice in experiment 2 were randomly assigned to 2 groups, receiving bilateral hippocampal injections of rAAV-empty or rAAV-ASIC1a ($n = 6$ /group). Animals were anesthetized with chloral hydrate (400 mg/kg, i.p.) and secured in a stereotaxic frame. rAAV-vectors ($2 \mu\text{L}$, 1.09×10^{12} – 1.15×10^{12} particles/mL) were injected bilaterally into the dentate gyrus (AP: -2.00 mm, LM: 1.40 mm, DV: 2.00 mm).

At the same time, polyimide-insulated silver wire monopolar depth electrodes (outside diameter 0.14 mm) were bilaterally implanted into CA1 (AP: -2.06 mm, LM: 1.60 mm, DV: 1.40 mm). A reference electrode was placed into the right frontal lobe (AP: 1.20 mm, LM: 1.80 mm, DV: 0.50 mm). A ground electrode was placed in the prefrontal bone^{48,49}. Each electrode was soldered to a single socket contact and attached to a plug using dental cement.

All experimental animals survived during rAAV injection period and EEG electrode implantation period. Then, continuous video-EEG monitoring was performed to record the change of EEG and behavior seizures on the 5th week after SE.

Continuous video-EEG monitoring and behavioral analysis. During the 5th week post-SE, animals were continuously monitored for 12 hours/day by video-EEG. EEG activity from hippocampal electrodes was amplified, filtered (high pass: 0.1 Hz; low pass: 45 Hz), and recorded (100 Hz sampling rate) with an EEG Amplifier System (SOLAR3000N, China). EEG seizures were defined as the paroxysmal activity of high frequency (>5 Hz) and amplitude (3-fold greater than baseline) lasting more than 20 s⁵⁰. Spontaneous behavioral seizures corresponded to paroxysmal alterations in the EEG recording⁵¹. Seizure severity was scored on the Racine scale based on the video recording⁵².

Video-EEG recordings were examined and analyzed by two independent, blinded investigators. In the event of different evaluations, investigators reviewed the recordings together to reach a consensus.

Patient evaluation and tissue preparation. Four refractory TLE patients (2 men, 2 women, mean age 22.75 ± 8.85 years, mean TLE history 14 ± 4.32 years) with unilateral hippocampal sclerosis identified by MRI were included in this study. The diagnosis was made by previously reported clinical and electrographic characteristics (Commission on Classification and Terminology of the International League Against Epilepsy, 1989). Four control patients, 3 men, 1 woman, mean age 32.2 ± 8.6 years, with traumatic brain injury caused by car accidents, were included in this study. All patients had undergone decompression surgery within six hours post-traumatic brain injury, and then parts of hippocampi were carefully isolated from tissues resected. Surgically resected sclerotic hippocampal tissue was dissected and fixed in 4% paraformaldehyde overnight at 4 °C. Specimens were embedded in paraffin after gradient alcohol dehydration. Paraffin-embedded brains were cut into 5 μm sections for immunofluorescence staining following standard laboratory procedures. The use of human tissue samples were approved by the Ethics Committee of Xijing Hospital. The patients provided written informed consent.

Primary culture of cortical astrocytes. The cerebral cortex was isolated from one-day-old C57BL/6J pups. Cells were dissociated by pipetting and trypsinization (0.125% trypsin with 0.02% EDTA, 15 minutes). Trypsinization was arrested with 1 mL trypsin inhibitor (0.125 mg/mL; Sigma). The suspension was then centrifuged (800 rpm, 5 minutes) and cells were resuspended in DMEM/F-12 (Invitrogen) supplemented with 15% fetal bovine serum (FBS). Cultured cells were maintained at 37 °C in humidified 95% oxygen/5% CO₂. At approximately 14 days *in vitro*, primary astrocytes were shaken at 280 rpm overnight to remove non-astrocytic cells. Purified astrocytes were used for experiments after two passages.

Immunofluorescence staining. Immunofluorescence staining was performed as previously described⁴⁶. Briefly, frozen sections or cells were incubated with anti-ASIC1a goat polyclonal (1:50, Santa Cruz) and anti-GFAP mouse monoclonal (1:3000, Sigma) antibodies overnight at 4 °C, followed by the appropriate secondary antibodies (1:500; Cell Signaling) for 2 hours at room temperature. Nuclei were counterstained with Hoechst 33258 for 5 minutes at room temperature. Frozen sections or cells were imaged on a confocal microscope (FV1000, Olympus, Japan). ASIC1a/GFAP immunofluorescence analysis was performed as described previously^{46,53}. Five coronal hippocampal sections were selected from each mouse. Total numbers of GFAP⁺ or ASIC1a⁺ cells were counted in a $5 \times 10^4 \mu\text{m}^2$ area.

Immuno-electron microscopy. Brain tissue immunogold staining was performed as described previously⁵⁴. Briefly, after fixing, dehydrating, saturating and embedding, coronal sections (70 nm) were incubated with anti-ASIC1a goat polyclonal (1:50, Santa Cruz) or anti-GFAP mouse monoclonal (1:3000, Sigma) antibodies overnight at 4 °C. Sections were then incubated with colloidal gold (5 nm or 10 nm)-conjugated secondary antibodies (rabbit anti-goat and anti-mouse IgG (Amersham)) for 2 hours at room temperature. Sections were rinsed with distilled water, dyed with 1% PVA containing 0.1% uranyl acetate, dried, then imaged using a Transmission Electron Microscope (Hitachi7500, Japan).

Western Blot analysis. Briefly, tissue or cells were lysed in RIPA buffer containing 2% protease inhibitor (Gibco). Lysates were separated on SDS-polyacrylamide gels and transferred to PVDF membranes (Millipore). Membranes were incubated with primary antibodies (goat anti-ASIC1a 1:200, Santa Cruz) and HRP-conjugated secondary antibodies (mouse anti-goat, 1:3000, Millipore), then developed with ECL (Millipore). Band intensities were quantified using Image-ProPlus 6.0 software. ASIC1a band intensity was normalized to GAPDH as a loading control.

Ca²⁺ imaging. Ca²⁺ imaging was performed as described previously^{54,55}. Briefly, cultured astrocytes were pre-treated with LPS (2 $\mu\text{g}/\text{ml}$) for 24 hours, then incubated with 5 μM fura-4 (Sigma-Aldrich) in PBS for 30 minutes at 37 °C. Fura-4 fluorescence was excited using a 494 nm laser line and emitted using a wavelength of 516 nm by an inverted microscope (Olympus, FV1000). Digitized images were acquired and analyzed in a PC controlled by FV10-ASW 3.1. Ratio images were analyzed by averaging pixel ratio values in circumscribed regions of cells in the field of view. The values were exported to Origin 8.0 for additional analysis.

Statistical analysis. All data are expressed as mean \pm SEM. Statistical comparisons were performed using Student's *t* tests or one-way ANOVAs with Dunnett's post-hoc test, as indicated. All statistical analyses were performed using SPSS v16.0. *P* values below 0.05 were considered statistically significant.

References

- Pitkanen, A. & Lukasiuk, K. Mechanisms of epileptogenesis and potential treatment targets. *Lancet Neurol* **10**, 173–186 (2011).
- Franco, V., French, J. A. & Perucca, E. Challenges in the clinical development of new antiepileptic drugs. *Pharmacol Res*, **103**, 95–104 (2015).
- Hubbard, J. A., Hsu, M. S., Fiacco, T. A. & Binder, D. K. Glial cell changes in epilepsy: overview of the clinical problem and therapeutic opportunities. *Neurochem Int* **63**, 638–651 (2013).
- Sendrowski, K. & Sobaniec, W. Hippocampus, hippocampal sclerosis and epilepsy. *Pharmacol Rep* **65**, 555–565 (2013).
- Gibbons, M. B., Smeal, R. M., Takahashi, D. K., Vargas, J. R. & Wilcox, K. S. Contributions of astrocytes to epileptogenesis following status epilepticus: opportunities for preventive therapy? *Neurochem Int* **63**, 660–669 (2013).
- Steinhauser, C., Grunnet, M. & Carmignoto, G. Crucial role of astrocytes in temporal lobe epilepsy. *Neuroscience*, **323**, 157–169 (2015).
- Crespel, A. *et al.* Inflammatory reactions in human medial temporal lobe epilepsy with hippocampal sclerosis. *Brain Res* **952**, 159–169 (2002).
- Boer, K. *et al.* Inflammatory processes in cortical tubers and subependymal giant cell tumors of tuberous sclerosis complex. *Epilepsy Res* **78**, 7–21 (2008).
- Vezzani, A., French, J., Bartfai, T. & Baram, T. Z. The role of inflammation in epilepsy. *Nat Rev Neurol* **7**, 31–40 (2011).

10. Friedman, A. & Dingledine, R. Molecular cascades that mediate the influence of inflammation on epilepsy. *Epilepsia* **52** Suppl 3, 33–39 (2011).
11. Chu, X. P., Papasian, C. J., Wang, J. Q. & Xiong, Z. G. Modulation of acid-sensing ion channels: molecular mechanisms and therapeutic potential. *Int J Physiol Pathophysiol Pharmacol* **3**, 288–309 (2011).
12. Mamet, J., Baron, A., Lazdunski, M. & Voilley, N. Proinflammatory mediators, stimulators of sensory neuron excitability via the expression of acid-sensing ion channels. *J Neurosci* **22**, 10662–10670 (2002).
13. Friese, M. A. *et al.* Acid-sensing ion channel-1 contributes to axonal degeneration in autoimmune inflammation of the central nervous system. *Nat Med* **13**, 1483–1489 (2007).
14. Chu, X. P. & Xiong, Z. G. Acid-sensing ion channels in pathological conditions. *Adv Exp Med Biol* **961**, 419–431 (2013).
15. Waldmann, R., Champigny, G., Bassilana, F., Heurteaux, C. & Lazdunski, M. A proton-gated cation channel involved in acid-sensing. *Nature* **386**, 173–177 (1997).
16. Yermolaieva, O., Leonard, A. S., Schnizler, M. K., Abboud, F. M. & Welsh, M. J. Extracellular acidosis increases neuronal cell calcium by activating acid-sensing ion channel 1a. *Proceedings of the National Academy of Sciences of the United States of America* **101**, 6752–6757 (2004).
17. Benarroch, E. E. Acid-sensing cation channels: structure, function, and pathophysiologic implications. *Neurology* **82**, 628–635 (2014).
18. Weng, J. Y., Lin, Y. C. & Lien, C. C. Cell type-specific expression of acid-sensing ion channels in hippocampal interneurons. *J Neurosci* **30**, 6548–6558 (2010).
19. Wemmie, J. A. *et al.* The acid-activated ion channel ASIC contributes to synaptic plasticity, learning, and memory. *Neuron* **34**, 463–477 (2002).
20. Huang, C. *et al.* Existence and distinction of acid-evoked currents in rat astrocytes. *Glia* **58**, 1415–1424 (2010).
21. Wang, Y. Z. *et al.* Tissue acidosis induces neuronal necroptosis via ASIC1a channel independent of its ionic conduction. *eLife* **4**, e05682 (2015).
22. Richichi, C. *et al.* Anticonvulsant and antiepileptogenic effects mediated by adeno-associated virus vector neuropeptide Y expression in the rat hippocampus. *The Journal of neuroscience: the official journal of the Society for Neuroscience* **24**, 3051–3059 (2004).
23. Perea, G., Navarrete, M. & Araque, A. Tripartite synapses: astrocytes process and control synaptic information. *Trends Neurosci* **32**, 421–431 (2009).
24. Colangelo, A. M., Alberghina, L. & Papa, M. Astroglialosis as a therapeutic target for neurodegenerative diseases. *Neurosci Lett* **565**, 59–64 (2014).
25. Yang, F. *et al.* Roles of astrocytes and microglia in seizure-induced aberrant neurogenesis in the hippocampus of adult rats. *Journal of neuroscience research* **88**, 519–529 (2010).
26. Sofroniew, M. V. & Vinters, H. V. Astrocytes: biology and pathology. *Acta Neuropathol* **119**, 7–35 (2010).
27. Eid, T. *et al.* Loss of perivascular aquaporin 4 may underlie deficient water and K⁺ homeostasis in the human epileptogenic hippocampus. *Proc Natl Acad Sci USA* **102**, 1193–1198 (2005).
28. Perea, G. & Araque, A. GLIA modulates synaptic transmission. *Brain Res Rev* **63**, 93–102 (2010).
29. Chu, X. P. & Xiong, Z. G. Physiological and pathological functions of acid-sensing ion channels in the central nervous system. *Curr Drug Targets* **13**, 263–271 (2012).
30. Ali, A., Ahmad, F. J., Pillai, K. K. & Vohora, D. Evidence of the antiepileptic potential of amiloride with neuropharmacological benefits in rodent models of epilepsy and behavior. *Epilepsy Behav* **5**, 322–328 (2004).
31. Ali, A., Pillai, K. P., Ahmad, F. J., Dua, Y. & Vohora, D. Anticonvulsant effect of amiloride in pentetrazole-induced status epilepticus in mice. *Pharmacol Rep* **58**, 242–245 (2006).
32. N'Gouemo, P. Amiloride delays the onset of pilocarpine-induced seizures in rats. *Brain Res* **1222**, 230–232 (2008).
33. Ou-Yang, T. P. *et al.* The Effects of Amiloride on Seizure Activity, Cognitive Deficits and Seizure-Induced Neurogenesis in a Novel Rat Model of Febrile Seizures. *Neurochem Res* **41**, 933–942 (2015).
34. Ziemann, A. E. *et al.* Seizure termination by acidosis depends on ASIC1a. *Nat Neurosci* **11**, 816–822 (2008).
35. Wei, D. *et al.* Degeneration and regeneration of GABAergic interneurons in the dentate gyrus of adult mice in experimental models of epilepsy. *CNS Neurosci Ther* **21**, 52–60 (2015).
36. Magloczky, Z. & Freund, T. F. Impaired and repaired inhibitory circuits in the epileptic human hippocampus. *Trends Neurosci* **28**, 334–340 (2005).
37. Cendes, F., Sakamoto, A. C., Spreafico, R., Bingaman, W. & Becker, A. J. Epilepsies associated with hippocampal sclerosis. *Acta Neuropathol* **128**, 21–37 (2014).
38. Wu, H. *et al.* Altered Expression Pattern of Acid-Sensing Ion Channel Isoforms in Piriform Cortex After Seizures. *Molecular neurobiology*, **53**, 1782–1793 (2016).
39. Cao, Q. *et al.* Elevated Expression of Acid-Sensing Ion Channel 3 Inhibits Epilepsy via Activation of Interneurons. *Mol Neurobiol* **53**, 485–498 (2016).
40. Fassler, M. *et al.* Preferential lentiviral targeting of astrocytes in the central nervous system. *PLoS One* **8**, e76092 (2013).
41. Merienne, N., Le Douce, J., Faivre, E., Deglon, N. & Bonvento, G. Efficient gene delivery and selective transduction of astrocytes in the mammalian brain using viral vectors. *Front Cell Neurosci* **7**, 106 (2013).
42. Murlidharan, G., Samulski, R. J. & Asokan, A. Biology of adeno-associated viral vectors in the central nervous system. *Front Mol Neurosci* **7**, 76 (2014).
43. Yan, Y. *et al.* CNS-specific therapy for ongoing EAE by silencing IL-17 pathway in astrocytes. *Molecular therapy: the journal of the American Society of Gene Therapy* **20**, 1338–1348 (2012).
44. Knopp, A., Frahm, C., Fidzinski, P., Witte, O. W. & Behr, J. Loss of GABAergic neurons in the subiculum and its functional implications in temporal lobe epilepsy. *Brain* **131**, 1516–1527 (2008).
45. Goffin, K., Nissinen, J., Van Laere, K. & Pitkanen, A. Cyclicity of spontaneous recurrent seizures in pilocarpine model of temporal lobe epilepsy in rat. *Exp Neurol* **205**, 501–505 (2007).
46. Meng, X. *et al.* Specific gene expression in mouse cortical astrocytes is mediated by a 1740bp-GFAP promoter-driven combined adeno-associated virus 2/5/7/8/9. *Neuroscience letters* **593**, 45–50 (2015).
47. Brenner, M., Kisseberth, W. C., Su, Y., Besnard, F. & Messing, A. GFAP promoter directs astrocyte-specific expression in transgenic mice. *The Journal of neuroscience: the official journal of the Society for Neuroscience* **14**, 1030–1037 (1994).
48. Lee, E. F., Jacobs, R. E., Dinov, I., Leow, A. & Toga, A. W. Standard atlas space for C57BL/6J neonatal mouse brain. *Anat Embryol (Berl)* **210**, 245–263 (2005).
49. El-Hayek, Y. H. *et al.* Hippocampal excitability is increased in aged mice. *Exp Neurol* **247**, 710–719 (2013).
50. Williams, P. A. *et al.* Development of spontaneous recurrent seizures after kainate-induced status epilepticus. *The Journal of neuroscience: the official journal of the Society for Neuroscience* **29**, 2103–2112 (2009).
51. Brandt, C., Nozadze, M., Heuchert, N., Rattka, M. & Loscher, W. Disease-modifying effects of phenobarbital and the NKCC1 inhibitor bumetanide in the pilocarpine model of temporal lobe epilepsy. *The Journal of neuroscience: the official journal of the Society for Neuroscience* **30**, 8602–8612 (2010).
52. Racine, R. J. Modification of seizure activity by electrical stimulation. II. Motor seizure. *Electroencephalogr Clin Neurophysiol* **32**, 281–294 (1972).

53. Arisi, G. M. *et al.* Astrocyte Alterations in the Hippocampus Following Pilocarpine-induced Seizures in Aged Rats. *Aging and disease* **2**, 294–300 (2011).
54. Akagi, T. *et al.* Improved methods for ultracryotomy of CNS tissue for ultrastructural and immunogold analyses. *Journal of neuroscience methods* **153**, 276–282 (2006).
55. Duan, B. *et al.* Extracellular spermine exacerbates ischemic neuronal injury through sensitization of ASIC1a channels to extracellular acidosis. *The Journal of neuroscience: the official journal of the Society for Neuroscience* **31**, 2101–2112 (2011).

Acknowledgements

This work was supported by grants from The National Science Foundation of China (No. 81271432 and 81571262). The funders had no role in study design, data collection and analysis, decision to publish, or preparation of the manuscript.

Author Contributions

W.J. conceived the study, designed experiments, and revised the article. F.Y., X.S. and Y.D. wrote the article. F.Y. and H.M. performed virus injection, video-EEG monitoring and behavioral experiments. Y.D. and X.S. performed western blotting, immunocytochemistry, and Ca^{2+} imaging experiments. T.O.Y., Y.M. and W.L. collected and analyzed data for video-EEG monitoring and behavioral experiments. T.X. provided ASIC1a knockout mice and related technology. All authors were participants in the discussion of results, and approved the final manuscript.

Additional Information

Competing financial interests: The authors declare no competing financial interests.

How to cite this article: Yang, F. *et al.* Astrocytic Acid-Sensing Ion Channel 1a Contributes to the Development of Chronic Epileptogenesis. *Sci. Rep.* **6**, 31581; doi: 10.1038/srep31581 (2016).



This work is licensed under a Creative Commons Attribution 4.0 International License. The images or other third party material in this article are included in the article's Creative Commons license, unless indicated otherwise in the credit line; if the material is not included under the Creative Commons license, users will need to obtain permission from the license holder to reproduce the material. To view a copy of this license, visit <http://creativecommons.org/licenses/by/4.0/>

© The Author(s) 2016